International Journal of Mechanical, Industrial and Aerospace Sciences
ISSN: 2517-9950
Vol:11, No:9, 2017

Modeling of Electrokinetic Mixing in Lab on Chip Microfluidic Devices

Virendra J. Majarikar, Harikrishnan N. Unni

***Abstract*—**This paper sets to demonstrate a modeling of electrokinetic mixing employing electroosmotic stationary and time-dependent microchannel using alternate zeta patches on the lower surface of the micromixer in a lab on chip microfluidic device. Electroosmotic flow is amplified using different 2D and 3D model designs with alternate and geometric zeta potential values such as 25, 50, and 100 mV, respectively, to achieve high concentration mixing in the electrokinetically-driven microfluidic system. The enhancement of electrokinetic mixing is studied using Finite Element Modeling, and simulation workflow is accomplished with defined integral steps. It can be observed that the presence of alternate zeta patches can help inducing microvortex flows inside the channel, which in turn can improve mixing efficiency. Fluid flow and concentration fields are simulated by solving Navier-Stokes equation (implying Helmholtz-Smoluchowski slip velocity boundary condition) and Convection-Diffusion equation. The effect of the magnitude of zeta potential, the number of alternate zeta patches, etc. are analysed thoroughly. 2D simulation reveals that there is a cumulative increase in concentration mixing, whereas 3D simulation differs slightly with low zeta potential as that of the 2D model within the T-shaped micromixer for concentration 1 mol/m^3 and 0 mol/m^3, respectively. Moreover, 2D model results were compared with those of 3D to indicate the importance of the 3D model in a microfluidic design process.

***Keywords*—**COMSOL, electrokinetic, electroosmotic, microfluidics, zeta potential.

I. Introduction

ELECTROKINETICS refers to the fluid/particles transport in the presence of an applied electric field [1], [2]. The applications of electrokinetics in advances of microfluidic devices have been a boon not only to the medical but also to the interdisciplinary fields. Moreover, it serves as a feasible tool in inventing a *lab-on-a-chip* for use in biological and chemical assays, manipulating fluids for several scientific and industrial contexts in the past decades.

The history of electrokinetics [3] can be traced back to the early 19th century where Reuss first studied the mixture of water/clay, and accordingly, demonstrated the electrokinetic effect using direct current (DC). Throughout the mid-19th century, numerous discoveries concerning the electrokinetics were established; however, in the most prominent discovery in 1879, Helmholtz developed the electrokinetic-based analytical model, and consequently, a combination of work between Pellat and Smoluchowski derived the velocity associated with the electrokinetic using the Helmholtz model as reference, and Casagrande demonstrated the electrokinetic phenomena using the soil as a porous media.

Under the effect of an employed electric field, electroosmosis [1], [4] refers to the fluid flow through a loosely attached particle, a pervious form, or a layer. In the other words, it is the movement of electrolytes within the fluid with respect to the fixed charged layer by an applied electric field. This electroosmotic phenomenon results into the moving ions strongly pulling the liquid, in which they are ingrain, owing to the force exerted under the influence of the electric field on the opposite charges in the fluid within the charged microchannel or tube. In addition, the charge balance between an electrolyte and solid active surface near the interface leading to the mobile ions film with the net electrical charges is linked to electrical double layer [5]. Also, the Coulomb force on charges in the interfacial layer, formed by an exerted electric potential result in the development of electroosmotic flow [6], [7], whereas the volume flow rate associated with the liquid distant from the charged interface is linked to electroosmotic velocity [8].

Microfluidics refers to manipulation of fluids at sub millimeter scales [9], [10] and delivers greater efficiency in existing processes such as smaller sample and fluid, quick output, faster arrangements, and easy processing. It comprises studying how the performance of the fluids at the microscale varies, and consequently, how they can be utilized for new use by integrating various microfluidic factors such as surface tension, energy dissipation, mobility under pressure, and fluidic interaction, etc. Additionally, mixer designs containing repeated stretching, curved and twisted channels [11], heterogeneous and homogeneous [12] combination surface patch, and fluid elements folding within the microfluidic mixing arms result in improving the efficiency of micromixers. Nevertheless, an effective microfluidic system must deliver greater contact efficiency, quick result, rapid and effective mixing, no undesirable reactions and contradictions irrespective of it geometric design. For higher mixing efficiency, the microfluidic devices can involve two processes; mainly, passive mixing [13] where the efficient mixing is achieved in pressure-driven micromixer incorporating different layers, configuration, and untoward event, whereas active mixing [14] involves in the application of external force field (e.g. electric potential field) within the micromixer in order to achieve fast and efficient mixing.

The magnitude of electroosmotic flow velocity is

Virendra J. Majarikar was with the Department of Biomedical Engineering, Indian Institute of Technology Hyderabad, Sangareddy, Telangana 502285 India. He is now with the Department of Materials Engineering, The University of Tokyo, Tokyo 113-8654 Japan (phone: +81-80-8144-6545; e-mail: majarikar@bionano.t.u-tokyo.ac.jp).

Harikrishnan N. Unni is with the Department of Biomedical Engineering, Indian Institute of Technology Hyderabad, Sangareddy, Telangana 502285 India (e-mail: harikrishnan@iith.ac.in).

correlated with zeta potential [15] and it can play an important role for the fluids mixing. The present study focuses on the effect of distribution zeta potential patches (that can be experimentally implemented by channel surface modification) and magnitude of zeta potential on electroosmotic flow field and concentration field (thus mixing efficiency).

II. Methodology

Numerical simulation has been performed in COMSOL Multiphysics® 5.0 software [16] for modeling of electrokinetic mixing, which uses a numerical method called the finite element method. It analyses the finite elements and segments a large numerical part into smaller elements by engaging defined equations and subsequent model the entire problem into a larger system. Here, the fluid flow and mass transport equations were simulated by using COMSOL 5.0, with the choice of appropriate boundary conditions. Simulation workflows such as setting up the model dimension and geometry, incorporating suitable material and meshing were selected.

A. Model Design

Figs. 1 and 2 show the respective 2D and 3D T-shaped micromixer template designs with two inlets for 1 mol/m^3 and 0 mol/m^3 concentration and single outlet to achieve effective mixing with 0.5 mol/m^3 concentration. Microchannel height for 2D and 3D design is 10 µm and 30 µm, respectively.

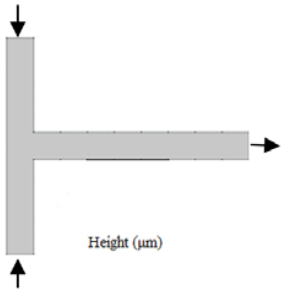

Fig. 1 2D T-shaped micromixer template design

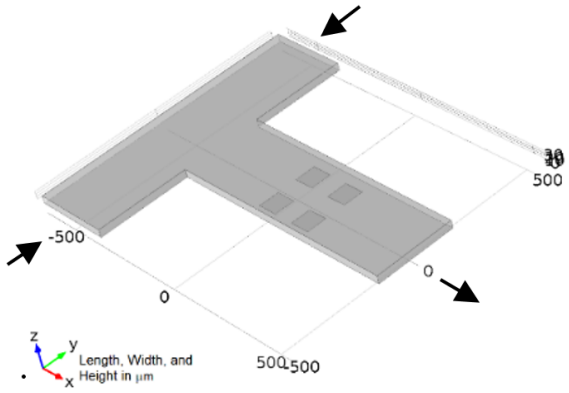

Fig. 2 3D T-shaped micromixer template design

B. Model Parameter

Electrokinetically-driven concentration mixing has been achieved by incorporating a set of simulation parameters which govern the fluid flow, fluid composition, physicochemical properties, etc. The model parameters have been selected to study effect of physicochemical parameters (mentioned in previous paragraphs) on micromixing efficiency (some default parameters defined within COMSOL Multiphysics®). Table I shows the numerical data on model parameter applied within the 2D and 3D T-shaped micromixer.

TABLE I
Data on Model Parameter

Symbol	Expression	Value	Description
u	0.1 (mm/s)	10^{-4} (m/s)	Mean inflow velocity
σ	2 (S/m)	2 (S/m)	Conductivity of the ionic solution
ε_r	45	45	Relative permittivity of the fluid
ζ	25 or 50 or 100 (mV)	25 or 50 or 100 (mV)	Zeta potential of the fluid
V	25 or 50 or 100 (mV)	25 or 50 or 100 (mV)	Applied electric potential value
Ω	2·pi(rad)·8 (Hz)	50.265 (Hz)	Angular frequency of the electric potential
D	10^{-11} (m^2/s)	10^{-11} (m^2/s)	Diffusion coefficient of the ionic solution
c	1 (mol/m^3)	1 (mol/m^3)	Initial concentration
t	0 (s)	0 (s)	Start time

C. Model Physics

To test simulation model, a set of physical interfaces has been coupled within designed microfluidic micromixer. The coupling between the defined physics and simulation equations helps to modify the analysis within test model. In order to perform physical modeling of 2D and 3D T-shaped model design, model physics such as laminar flow, electric current, and transport of diluted species are applied. At a slower rate, laminar fluid moves in straight and equidistant layers without turbulent mixing, whereas transport of diluted species is due to the flux and concentration gradients in the fluids.

D. Model Meshing

COMSOL Multiphysics® 5.0 provides various meshing element for electroosmotic simulation. The 2D model designs incorporate triangular and quadrilateral mesh, whereas 3D model involves tetrahedral, pyramid, brick, and prism. Tetrahedral element represents the simplex 3D default element type within COMSOL Multiphysics with adaptive mesh refinement whereas the other three elements types, i.e. pyramid, brick, and prism involves high meshing algorithm and user input, and sometimes unable to mesh a particular geometry. 2D model environment consists of 22 vertex elements, 22 boundary elements, 20 element number, 0.2 maximum element size, 1.1 maximum element growth size, and 0.005468 minimum element quality with triangular mesh, whereas 3D model environment consists of around 300000 elements and 1100000 degrees of freedom, 64 vertex elements, and around 2500 edge elements with tetrahedral mesh. In addition, higher mesh density is provided near the zeta patch both in 2D and 3D models in order to take into account of variations in solution. Table II shows the data on the 3D mesh size observed during numerical simulation.

TABLE II
DATA ON 3D MESH SIZE

Mesh Character	Value
Maximum element size	130
Minimum element size	2
Curvature factor	0.6
Resolution of narrow regions	0.5
Maximum element growth rate	1.5
Custom element size	Custom

E. Governing Equation

During the modeling of electrokinetic mixing using electroosmotic flow, certain definite simulation equations which were coupled to achieve the maximum concentration mixing among two different concentration solutions are as follows:

The Navier-Stokes equation for incompressible flow [17] describing the flow in the channel is expressed as

$$\rho\left[\frac{\partial v}{\partial t} + (v.\nabla)v\right] = -\nabla p + \mu\nabla^2 v + f \quad (1)$$

where $\rho\left[\frac{\partial v}{\partial t} + (v.\nabla)v\right]$ represents inertial term, $\frac{\partial v}{\partial t}$ represents unsteady acceleration, $(v.\nabla)v$ represents convective acceleration, $-\nabla p$ is pressure gradient, $\mu\nabla^2 v$ is viscosity (kg/ms), f *is* is external force (kg.m/s^2), and ρ is fluid density (kg/m^3).

The combination of convection and diffusion effects within the micromixer contributes to the concentration gradients as well as the flux of the charged particles. The Convection-Diffusion equation [18] describing the concentration of the dissolved substances in the fluid inside the rectangular micromixer is expressed as

$$\frac{\partial C}{\partial t} + \nabla(-D\nabla C) = R - u\nabla C \quad (2)$$

where C is the concentration of the dissolved species (mol/m^3), $\frac{\partial C}{\partial t}$ is the concentration gradient, D is the diffusion coefficient of the solution, R is the reaction rate (here, $R = 0$ since concentration is not affected by any reactions), and u is the mean inflow velocity (mm/s).

The simulation model replaces the presence of thin electric double layer on channel wall with the Helmholtz-Smoluchowski [2], [18] relation, and Smoluchowski velocity is used explicitly as boundary condition along the channel wall, is expressed as

$$u = \frac{\varepsilon_r \varepsilon_0 \zeta V}{\eta} \quad (3)$$

where u represents the velocity (mm/s), ε_r is the relative permittivity (F/m), ε_0 is the fluid permittivity in free space (F/m), ζ is the zeta potential at the channel walls (mV), V the is electric potential (mV), and η is the dynamic viscosity (kg/ms).

III. RESULTS AND DISCUSSIONS

To demonstrate effective concentration mixing within the T-shaped micromixer, different 2D, as well as 3D, model designs were simulated.

A. 2D Model for Electrical Contour and Velocity Field Streamline within 10 µm Height Microchannel

Fig. 3 depicts 25 mV zeta potential with the low streamline velocity field, 50 mV with the slight increase, whereas 100 mV reveals the maximum streamline velocity field within 10 µm height micromixer for four alternate and opposite electric potential.

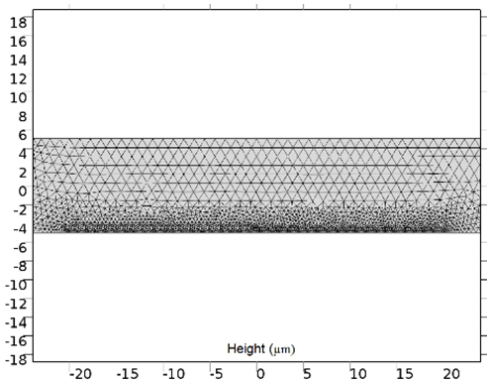

(a)

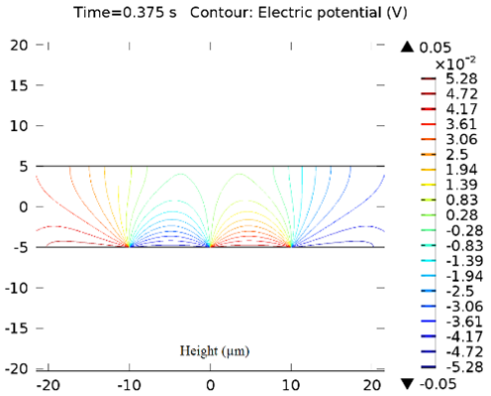

(b)

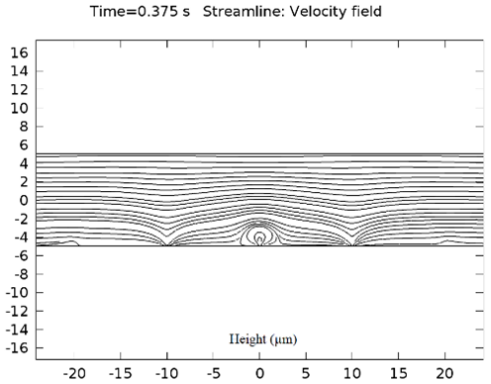

(c)

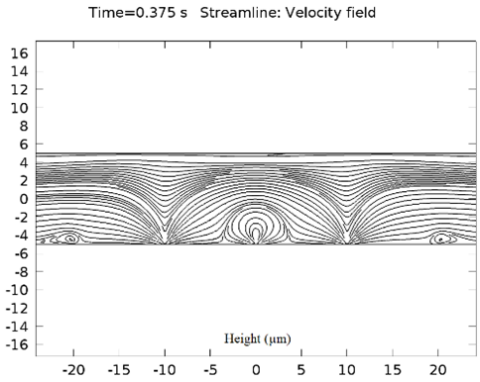

(d)

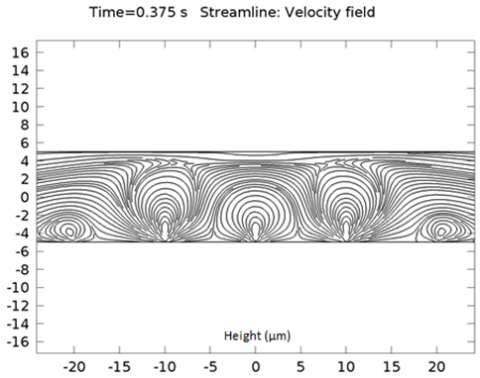

(e)

Fig. 3 2D model for electric contour and velocity field streamline within 10 μm height microchannel. (a) Microchannel triangular meshing. (b) Electric potential contour. (c) Velocity field streamline of 25 mV zeta potential. (d) Velocity field streamline of 50 mV zeta potential. (e) Velocity field streamline of 100 mV zeta potential

B. 2D T-Shaped Micromixer for Surface Concentration Using Three Alternate and Opposite Potential within 10 μm Height Microchannel

Fig. 4 depicts 1 mol/m^3 and 0 mol/m^3 concentration mixing within 10 μm height micromixer using three alternate and opposite electric potential. 25 mV zeta potential shows low mixing, 50 mV with the slight increase, whereas 100 mV displays close to (0.5 mol/m^3) complete mixing.

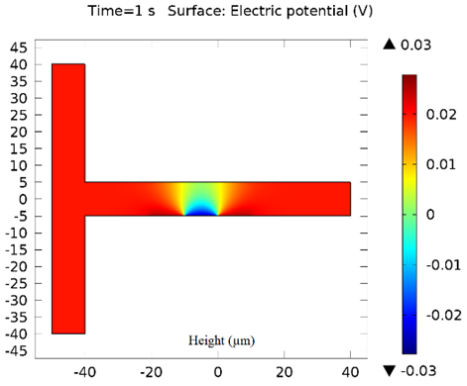

(a)

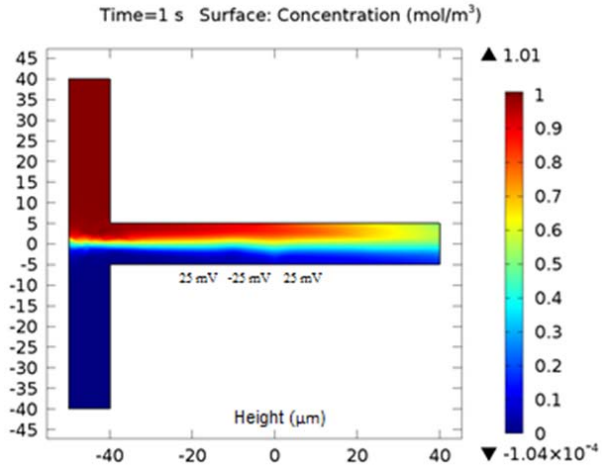

(b)

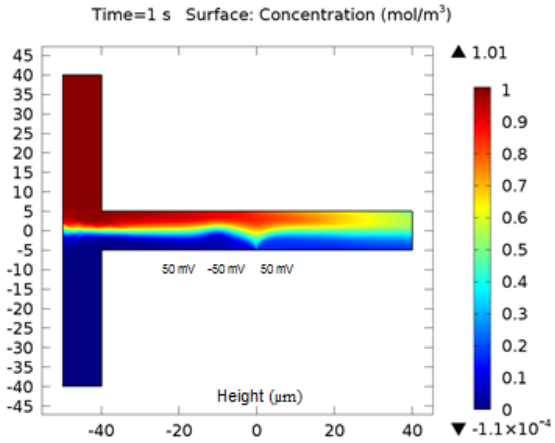

(c)

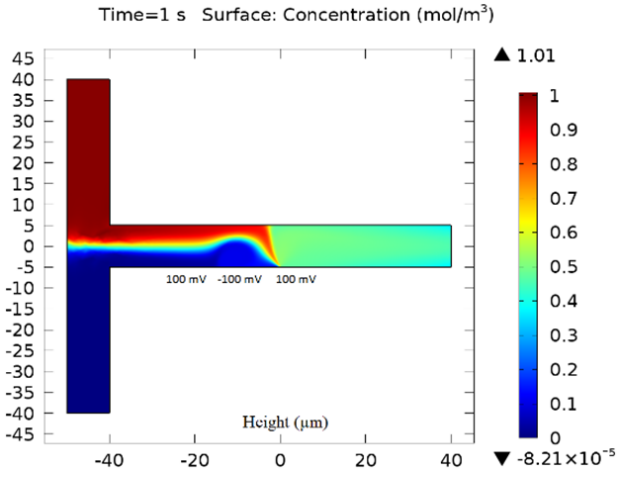

(d)

Fig. 4 2D model with three alternate and opposite electric potential within 10 μm height microchannel. (a) Microchannel with three electric potentials. (b) Surface concentration with 25 mV electric potential. (c) Surface concentration with 50 mV electric potential. (d) Surface concentration with 100 mV electric potential

C. 2D T-Shaped Micromixer for Surface Concentration Using Four Alternate and Opposite Potential within 10 µm Height Microchannel

Fig. 5 depicts the 2D T-shaped micromixer with four alternate and opposite electric potential having same simulation results as that of three alternate and opposite electric potential micromixer.

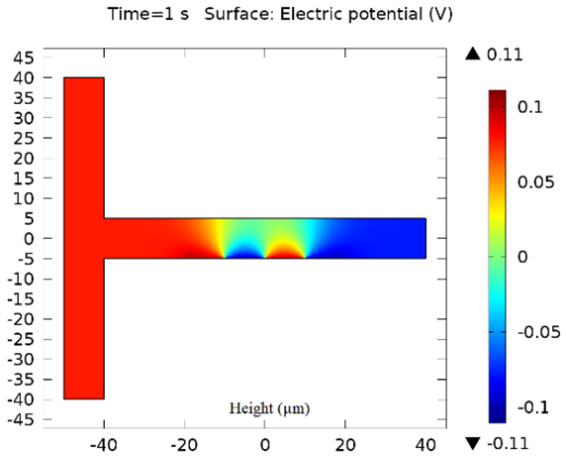

(a)

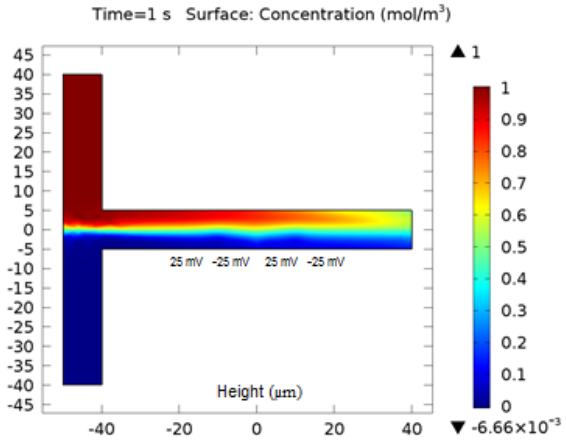

(b)

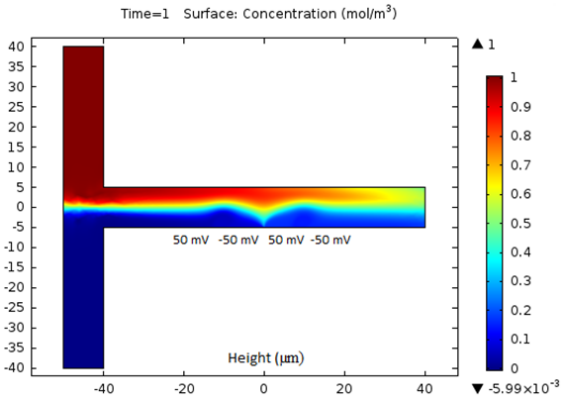

(c)

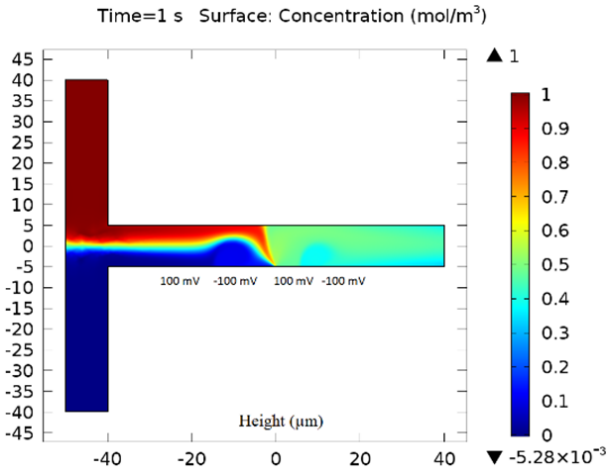

(d)

Fig. 5 2D model with four alternate and opposite electric potential within 10 µm height microchannel. (a) Microchannel with four electric potentials. (b) Surface concentration with 25 mV electric potential. (c) Surface concentration with 50 mV electric potential. (d) Surface concentration with 100 mV electric potential

D. 3D T-Shaped Micromixer for Surface Concentration Using Four Zeta Patches of Opposite Electric Potential within 30 µm Height Microchannel

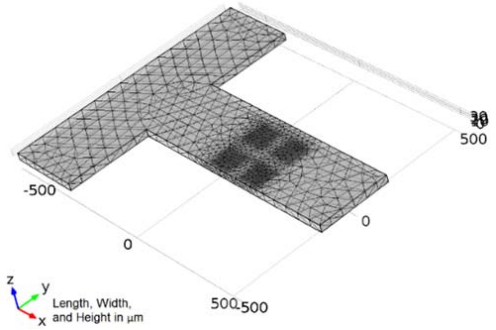

(a)

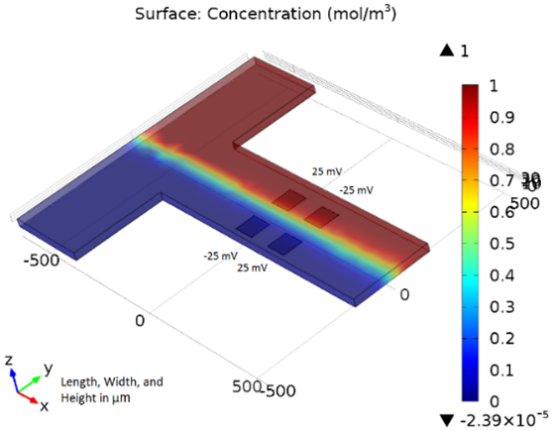

(b)

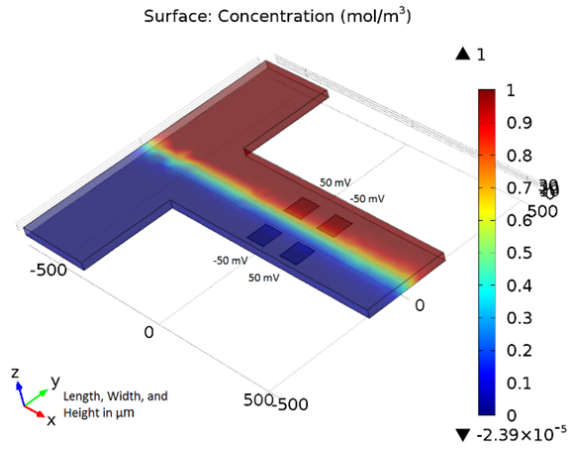

(c)

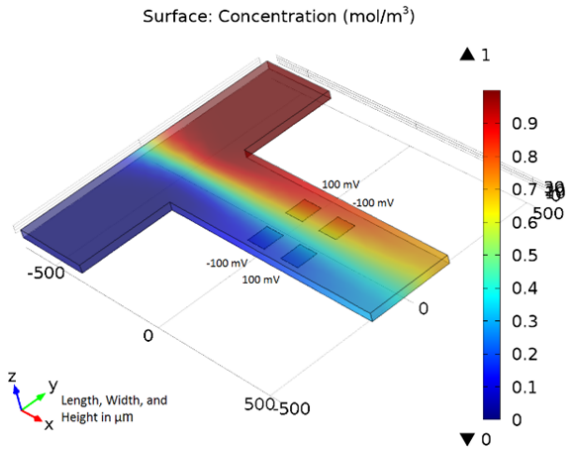

(d)

Fig. 6 3D model with four zeta patches of opposite electric potential within 30 µm height microchannel. (a) Microchannel with tetrahedral meshing. (b) Surface concentration with 25 mV electric potential. (c) Surface concentration with 50 mV electric potential. (d) Surface concentration with 100 mV electric potential

Fig. 6 depicts the 3D T-shaped micromixer with four zeta patches of opposite electric potential. 25 mV, 50 mV, and 100 mV zeta potentials show poor mixing within 30 µm height micromixer for 1 mol/m^3 and 0 mol/m^3 concentration.

E. 3D T-Shaped Micromixer for Surface Concentration Using Six Zeta Patches of Opposite Electric Potential within 30 µm Height Microchannel

Fig. 7 depicts the 3D T-shaped micromixer with six zeta patches of opposite electric potential. 25 mV and 50 mV zeta potentials show poor mixing, whereas 100 mV displays close to (0.5 mol/m^3) complete mixing within 30 µm height micromixer for 1 mol/m^3 and 0 mol/m^3 concentration.

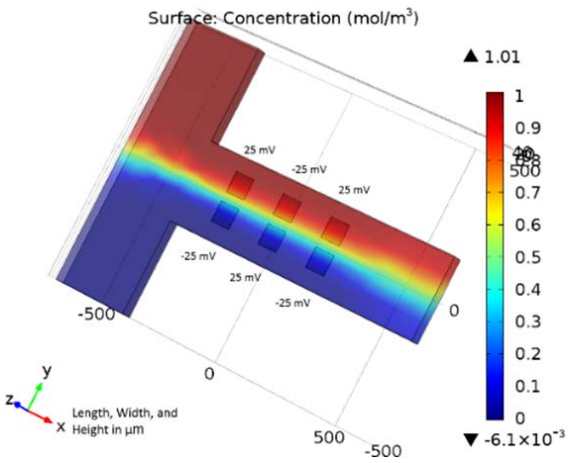

(a)

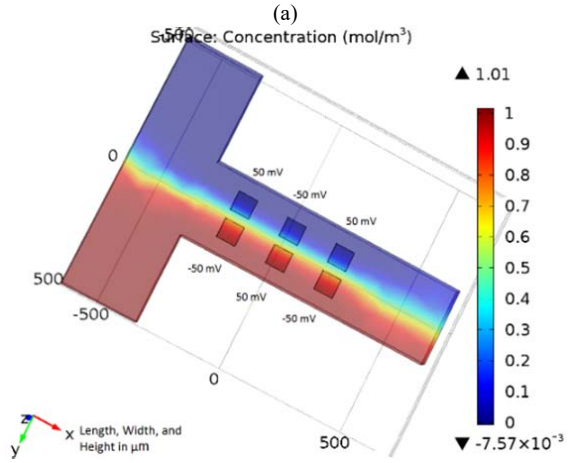

(b)

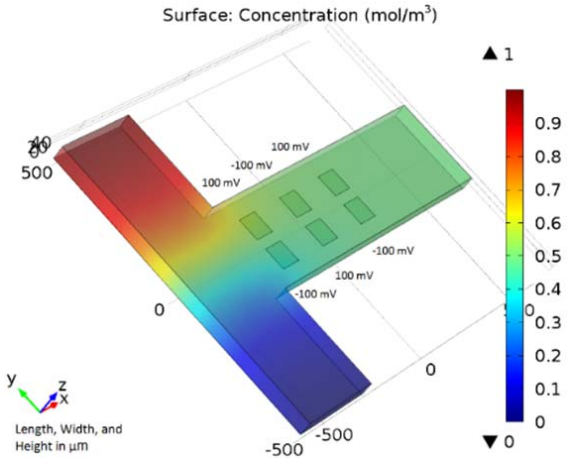

(c)

Fig. 7 3D model with six zeta patches of opposite electric potential within 30 µm height microchannel. (a) Surface concentration with 25 mV electric potential. (b) Surface concentration with 50 mV electric potential. (c) Surface concentration with 100 mV electric potential

F. 3D T-Shaped Micromixer for Surface Concentration Using Eight Zeta Patches of Opposite Electric Potential within 30 μm Height Microchannel

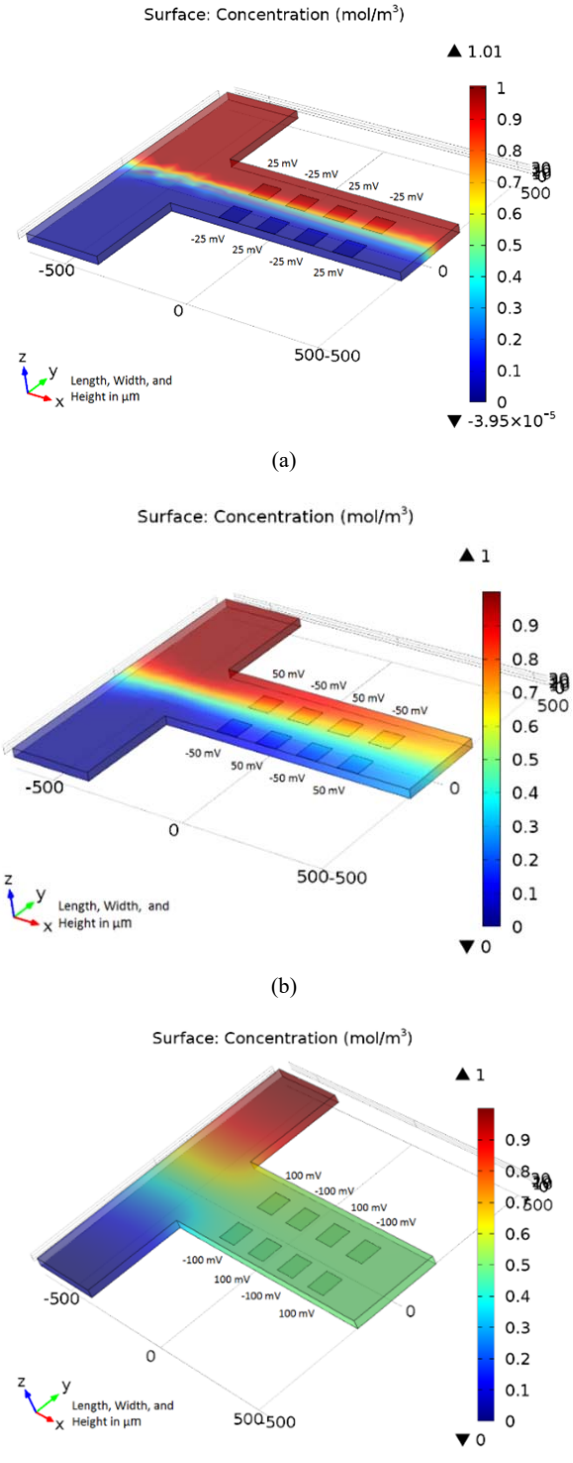

Fig. 8 3D model with eight zeta patches of opposite electric potential within 30 μm height microchannel. (a) Surface concentration with 25 mV electric potential. (b) Surface concentration with 50 mV electric potential. (c) Surface concentration with 100 mV electric potential

Fig. 8 depicts the 3D T-shaped micromixer with eight zeta patches of opposite electric potential. 25 mV zeta potential shows poor mixing, 50 mV with the slight increase, whereas 100 mV displays close to (0.5 mol/m^3) complete mixing within 30 μm height micromixer for 1 mol/m^3 and 0 mol/m^3 concentration.

G.3D T-Shaped Micromixer for Isosurface Concentration Using Eight Zeta Patches of Opposite Electric Potential within 30 μm Height Microchannel

Fig. 9 depicts the isosurface concentration plot for 3D T-shaped micromixer with eight zeta patches of opposite electric potential.

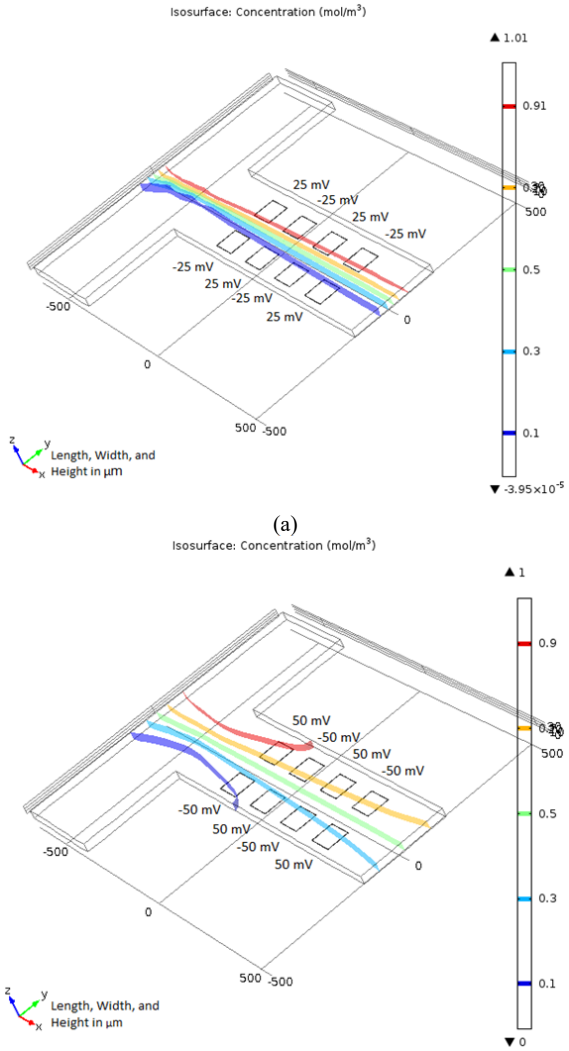

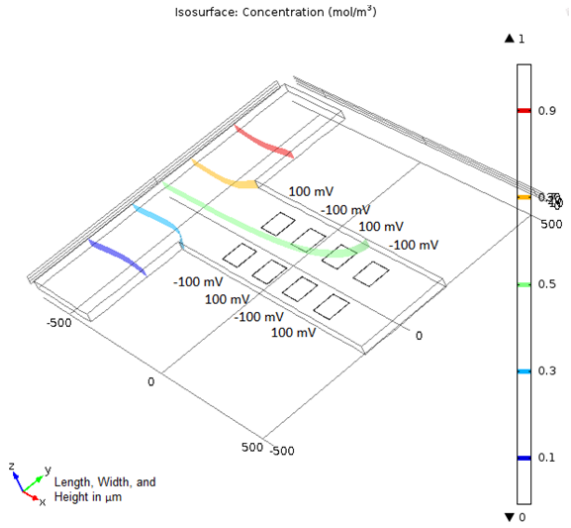

(c)

Fig. 9 3D model with eight zeta patches of opposite electric potential within 30 µm height microchannel. (a) Isosurface concentration with 25 mV electric potential. (b) Isosurface concentration with 50 mV electric potential. (c) Isosurface concentration with 100 mV electric potential

IV. Conclusion

Numerical simulations have been performed to investigate the electrokinetic mixing using alternate zeta patches on the lower surface of the T-shaped mixing chamber in COMSOL Multiphysics®. 2D simulation result reveals that there is a cumulative increase in concentration mixing, 25 mV zeta potential show poor mixing, whereas 100 mV zeta potential displays close to (0.5 mol/ m^3) complete mixing. In 3D simulation using four and six zeta patches, 25 mV and 50 mV zeta potentials show poor mixing; however, with eight zeta patches, there has been a significant increase in 50 mV mixing efficiency. Moreover, close to complete mixing (0.5 mol/ m^3) is achieved in 100 mV using six and eight zeta patches for mixing 1 mol/ m^3 and 0 mol/m^3 concentrations. Henceforth, 3D simulation results show that a number of zeta patches and magnitude of zeta potential play a key role in determining mixing efficiency, where the strength of zeta potential becomes the key factor after the certain level of zeta patch organization.

It should also be indicated here that the effect of microchannel height is not considered in the present study; this could be another factor that regulates mixing. The reported work can be of help in developing electrokinetic microfluidic devices for biological analysis such as drug screening where the efficiency of analyte mixing is vital.

Acknowledgment

The authors are grateful to the Department of Biomedical Engineering, Indian Institute of Technology Hyderabad (IITH) for their immense support.

References

[1] C. C. Chang and R. J. Yang, "Electrokinetic mixing in microfluidic systems," *Microfluid Nanofluid*, vol. 3 (5), 2007, pp. 501–525.
[2] A. V. Delgado, F. Gonzalez-Caballero, R. J. Hunter, L. K. Koopal and J. Lyklema, "Measurement and interpretation of electrokinetic phenomena," *Journal of Colloid and Interface Science,* vol. 309 (2), 2007, pp. 194–224.
[3] S. Wall, "The history of electrokinetic phenomena," *Current Opinion in Colloid and Interface Science*, vol. 15 (3), 2010, pp. 119–124.
[4] C. C. Chang and R. J. Yang, "Computational analysis of electrokinetically driven flow mixing with patterned blocks," *J Micromech Microeng*, vol. 14, 2004, pp. 550–558.
[5] C. C. Chang and R. J. Yang, "Electroosmosis – a Mechanism of Micromixer and Micropump," *J Micromech Microeng,* 14, 2004, pp. 550.
[6] C. K. Chen and C. C. Cho, "Electrokinetically driven flow mixing utilizing chaotic electric fields," *Microfluid Nanofluid,* vol. 5 (6), 2008, pp. 785–793.
[7] F. R. Phelan, P. Kutty and J. A. Pathak, "An electrokinetic mixer driven by oscillatory cross flow," *Microfluid Nanofluid,* vol. 5 (1), 2008, pp. 101–118.
[8] D. Sinton, C. E. Canseco, L. Ren and D. Li, "Direct and Indirect Electroosmotic Flow Velocity Measurements in Microchannels," *Journal of Colloid and Interface Science*, vol. 254 (1), 2002, pp. 184–189.
[9] G. M. Whitesides, "The origins and the future of microfluidics," *Nature,* vol. 442, 2006, pp. 368–373.
[10] D. Mark, S. Haeberle, G. Roth, F. Stettenz and R. Zengerle, "Microfluidic lab-on-a-chip platforms: requirements, characteristics and applications," *Chem. Soc. Rev.,* vol. 39 (3), 2010, pp. 1153–1182.
[11] J. K. Chen, W. J. Luo and R. J. Yang, "Electroosmotic flow driven by DC and AC electric fields in curved microchannels," *Jap J Appl Phys* 45, 2006, pp. 7983–7990.
[12] D. Erickson and D. Li, "Influence of Surface Heterogeneity on Electrokinetically Driven Microfluidic Mixing," *Langmuir,* vol. 18 (5), 2002, pp. 1883-1892.
[13] R. F. Ismagilov, A. D. Stroock, P. A. Kenis, G. M. Whitesides and H. A. Stone, "Experimental and theoretical scaling laws for transverse diffusive broadening in two-phase laminar flow in microchannels," *Appl Phys* Lett, vol. 76 (17), 2000, pp. 2376–2378.
[14] S. Wiggins and J. M. Ottino, "Foundations of chaotic mixing," *Phil Trans R Soc Lond A,* vol. 362, 2004, pp. 937–970.
[15] R. J. Hunter, "Zeta potential in colloid science: principles and applications," *Academic Press*, New York, 1981.
[16] COMSOL Multiphysics, "Introduction to COMSOL Multiphysics," http://www.comsol. no/shared/downloads/Introduction COMSOL Multiphysics.pdf (accessed in August 2015).
[17] G. H. Tanga, L. Zhuo, J. K. Wang, Y. L. He and W. Q. Tao, "Electroosmotic flow and mixing in microchannels with the lattice Boltzmann method," *Journal of Applied Physics*, vol. 100, Issue 9, 2006, pp. 094908–094910.
[18] H. S. Seo, B. Han and Y. J. Kim, "Numerical Study on the Mixing Performance of a Ring-Type Electroosmotic Micromixer with Different Obstacle Configurations," *J. Nanosci. Nanotechnol.,* vol. 12 (6), 2012, pp. 4523–4530.